A Comparison of Vibration Control Strategies for a Flexible-Link Robot Arm

S. Andrew Gadsden

Department of Mechanical Engineering
Faculty of Engineering
University of Maryland, Baltimore County
gadsden@umbc.edu

Mohammad AlShabi

Department of Mechanical Engineering
Faculty of Engineering
University of Sharjah
malshabi@sharjah.ac.ae

ABSTRACT

Flexible links in a robot arm often experience unwanted vibrations at the end points typically due to elastic deflections and system disturbances. This leads to reduced endpoint positioning accuracy, as well as negatively affects the overall control performance of the robot arm. Typical control strategies introduce active damping to reduce oscillations at the robot arm end points, whereas other methods apply interaction strategies based on closed-loop inverse kinematics. Other controllers, such as proportional-integral-derivative (PID) methods and the robust sliding mode controller (SMC), have also been applied to robot arms in an effort to minimize endpoint vibration. This paper studies two popular vibration control strategies found in literature, namely PID and SMC. Simulation results are generated based on applications to a flexible-link robot arm, and the results are compared and discussed.

Keywords—flexible-link; robot arm; PID; sliding mode control; vibration control strategy

1. INTRODUCTION

The study of vibration isolation and control spans a wide variety of topics and applications. An important area of vibration control involves robotics and the corresponding end effectors [1, 2]. Flexible-link robots have a number of advantages over rigid-link robots [3, 4]. For example, flexible-link robots are generally more maneuverable, require less material, lower power consumption, consist of smaller sub-components, have a higher payload-to-weight ratio, and also have a less overall cost [5].

The PID controller is one of the most well-studied control strategies found in literature [6, 7, 8]. The PID controller has a wide range of applications, from washing machines to robotics [9, 10, 11]. It is popular due to its ease of implementation and relatively simple structure. Essentially, the PID controller makes use of a reference signal or desired trajectory. This trajectory is compared with the actual system output, and a corresponding error is calculated. This error is fed into the PID controller which provides an adjusted system input. This process is repeated iteratively. Another popular control strategy is variable structure control (VSC) theory [12, 13, 14, 15]. The most well-established VSC method is the sliding mode controller (SMC) [13, 16, 17]. As per [18], SMC utilizes a discontinuous switching plane along some desired trajectory. This trajectory is referred to as a sliding surface S. It attempts to model the performance in the state variable space. The main objective in SMC theory is to keep the state values close to the sliding surface such that the state errors are minimized [15]. The controller forces the state trajectories towards the sliding surface and keeps it within a region or subspace.

In this short paper, the PID and SMC strategies are applied on a flexible-link robot arm for the purposes of vibration control. Section 2 provides a summary of the main PID and SMC equations. The flexible-link robot arm is described in further detail in Section 3. The simulation results are compared and discussed in Section 4. Section 5 summarizes the main findings in the paper.

2. CONTROL STRATEGIES

A. PID Controller

The PID controller is based on tracking errors and a set of three parameters or gains. These gains are corresponding error are used to generate an input that should drive the system to follow the desired trajectory. The PID controller computes the system input as follows.

$$u(t) = K_P e(t) + K_I \int e(t)dt + K_D \frac{de(t)}{dt} \qquad (2.1.1)$$

$$e(t) = r(t) - y(t) \qquad (2.1.2)$$

where $u(t)$ is the control signal used by the system, $y(t)$ is the system output or measurement, and $e(t)$ is the corresponding error. The PID parameters or gains, referred to as K_P, K_I, and K_D, are typically tuned by trial-and-error. This process can be tedious, however there are some basic principles that, if understood, help to expedite the tuning process. The proportional gain typically reduces the rise time, however increases the amount of overshoot. The derivative gain reduces the overshoot present in the system, but increases the settling time. The integral gain generally is used to reduce the steady state error. All three gains are interconnected, and tuning one parameter has an effect on the other two.

B. Sliding Mode Control Strategy

Variable structure control (VSC) theory is a very robust control methodology [12]. The most well-established VSC method is the sliding mode controller (SMC) [13]. As per [18], SMC utilizes a discontinuous switching plane along some desired trajectory. This trajectory is referred to as a sliding surface S. It attempts to model the performance in the state variable space. The main objective in SMC theory is to keep the state values close to the sliding surface such that the state errors are minimized. The controller forces the state trajectories towards the sliding surface

978-1-4673-7797-3/15/$31.00 ©2015 IEEE

and keeps it within a region or subspace. The control law that satisfies the sliding condition is defined as follows:

$$s\dot{s} < 0 \qquad (2.2.1)$$

Equation (2.2.1) ensures that the sliding surface is forced towards the state space trajectory. The switching about the trajectory brings inherent stability to the control strategy. This switching effect is referred to as chattering. In an effort to minimize chattering, a saturation term or smoothing boundary region may be introduced.

As an example, consider a sliding surface for a third-order system, as follows:

$$S = \ddot{e} + 2\xi\lambda\dot{e} + \lambda^2 e \qquad (2.2.2)$$

where λ (>0) is the control bandwidth and ζ is the damping ratio [18]. Selecting a damping ratio ζ=1 results in critically damped closed-loop dynamics. In most cases, the SMC strategy requires a full state feedback. If excessive noise is present in the available measurements, the damping ratio should be selected as a small value, to minimize the effects of the noise.

A robust control law is created by combining the equivalent control component u_{eq} with a robust switching component u_{sw}, as follows [12]:

$$U = u_{eq} + u_{sw} \qquad (2.2.3)$$

where the equivalent control component is used to achieve the desired motion on the sliding surface. The switching components may be defined as follows:

$$\dot{S}, \dot{S}_{int} \rightarrow u_{eq} = \frac{\dddot{x}_d - \hat{f}(\boldsymbol{x}) - 2\lambda\xi\ddot{e} - \lambda^2\dot{e}}{\hat{b}(\boldsymbol{x})} \qquad (2.2.4)$$

$$u_{eq,int} = \frac{\dddot{x}_d - \hat{f}(\boldsymbol{x}) - (2\lambda\xi + \lambda)\ddot{e}}{\hat{b}(\boldsymbol{x})} - \frac{(2\lambda^2\xi + \lambda^2)\dot{e} + \lambda^3 e}{\hat{b}(\boldsymbol{x})} \qquad (2.2.5)$$

$$\hat{b}(\boldsymbol{x}) = \sqrt{b_{min}(\boldsymbol{x})b_{max}(\boldsymbol{x})} \qquad (2.2.6)$$

$$\hat{f}(\boldsymbol{x}) = \frac{f_{min}(\boldsymbol{x}) + f_{max}(\boldsymbol{x})}{2} \qquad (2.2.7)$$

where $\hat{f}(\boldsymbol{x})$ and $\hat{b}(\boldsymbol{x})$ are the nominal or estimate values of $f(\boldsymbol{x})$ and $b(\boldsymbol{x})$, respectively [18]. The switching control component that accommodates the model uncertainties and disturbances is defined as follows [12, 13]:

$$u_{sw} = -\frac{K_{SMC}}{\hat{b}(\boldsymbol{x})} sat\left(\frac{S}{\phi}\right), \quad where \qquad (2.2.8)$$

$$K_{SMC} \geq \beta(F(\boldsymbol{x}) + \eta) + (\beta - 1)\left|\hat{b}(\boldsymbol{x})u_{eq}\right| \qquad (2.2.9)$$

$$\beta = \sqrt{\frac{b_{max}(\boldsymbol{x})}{b_{min}(\boldsymbol{x})}} \qquad (2.2.10)$$

$$\left|f(\boldsymbol{x}) - \hat{f}(\boldsymbol{x})\right| \leq F(\boldsymbol{x}) = \alpha\hat{f}(\boldsymbol{x}) \qquad (2.2.11)$$

where β is the gain margin, $F(\boldsymbol{x})$ is the estimation error on $f(\boldsymbol{x})$, α is the uncertainty factor, and ϕ is the boundary layer thickness. Once the control signal has been calculated, it is fed into the system. The system outputs and corresponding state errors are used in the SMC method, and the process is repeated iteratively.

3. FLEXIBLE-LINK ROBOT ARM

The flexible-link robot arm studied in this paper is defined in [3, 6, 11]. Typically, a flexible-link robot arm or system can be mathematically modelled using two degrees of freedom (DOF). These DOF may be represented by θ and α, which refers to the rotation angle of the arm and the oscillation angle of the end effectors, respectively. The position of the end effectors or tip is calculated by combining both angles. In an ideal scenario, the oscillation angle due to the flexibility in the link is minimized. Desired trajectories and arm movement excite the motion and unwanted oscillations. It is the goal of the controller (e.g., PID or SMC) to minimize the tracking error between the desired and actual robot arm position.

According to [6], the system may be represented by an energy balance equation, defined by:

$$L = K - P \qquad (3.1)$$

where L, K, and P refer to the Lagrange, kinetic, and potential energies, respectively. The Lagrange motion equations are defined by the following [6]:

$$\frac{d}{dt}\frac{\partial L}{\partial \dot{\alpha}} - \frac{\partial L}{\partial \alpha} = 0 \qquad (3.2)$$

$$\frac{d}{dt}\frac{\partial L}{\partial \dot{\theta}} - \frac{\partial L}{\partial \theta} = \tau \qquad (3.3)$$

Furthermore, as per [6], the system motion may be described by:

$$J_l\ddot{\theta} + J_l\ddot{\alpha} + K_s\alpha - MGHsin(\theta + \alpha) = 0 \qquad (3.4)$$

$$(J_h + J_l)\ddot{\theta} + J_l\ddot{\alpha} - MGHsin(\theta + \alpha) = \tau \qquad (3.5)$$

The motor torque τ is related to the armature voltage v, which is considered the system input. As per [6], in this paper, the state vector is defined by:

$$x = \begin{bmatrix} \theta \\ \alpha \\ \dot{\theta} \\ \dot{\alpha} \end{bmatrix} \qquad (3.6)$$

The single flexible-link system equations with corresponding state variables is defined as follows:

$$\dot{x}_1 = x_3 \qquad (3.7)$$

$$\dot{x}_2 = x_4 \qquad (3.8)$$

$$\dot{x}_3 = \frac{K_s}{J_h}x_2 - \frac{K_m^2K_g^2}{R_mJ_h}x_3 + \frac{K_mK_g}{R_mJ_h}v \qquad (3.9)$$

$$\dot{x}_4 = -\frac{K_s}{J_h}x_2 + \frac{K_m^2K_g^2}{R_mJ_h}x_3 - \frac{K_mK_g}{R_mJ_h}v - \frac{K_s}{J_l}x_2 + \frac{MGH}{J_l}\sin(x_1 + x_2) \qquad (3.10)$$

Note that the system input u is the voltage v. The measurement or system output is the sum of the flexible joint rotation θ and end effector deflection angle α. The state space model is defined by the following equations [6]:

$$\dot{x} = f(x) + g(x)u \qquad (3.11)$$

$$y = x_1 + x_2 \qquad (3.12)$$

where the system and measurement functions are defined respectively by the following:

$$f(x) = \begin{bmatrix} x_3 \\ x_4 \\ \frac{K_s}{J_h}x_2 - \frac{K_m^2K_g^2}{R_mJ_h}x_3 \\ -\frac{K_s}{J_h}x_2 + \frac{K_m^2K_g^2}{R_mJ_h}x_3 - \frac{K_s}{J_l}x_2 + \frac{MGH}{J_l}\sin(x_1 + x_2) \end{bmatrix} \qquad (3.13)$$

The above equations summarize the flexible-link robot arm system, and are used to model the system in the simulation

4. SIMULATION RESULTS

A number of different scenarios were studied to highlight the differences between the PID and SMC strategies. Note that the time step used in the simulation was $1\ ms$. Furthermore, note that the system equations were formulated in a discrete-time, as follows:

$$x_{1,k+1} = Tx_{3,k} + x_{1,k} \qquad (3.15)$$

$$x_{2,k+1} = Tx_{4,k} + x_{2,k} \qquad (3.16)$$

$$x_{3,k+1} = \frac{K_s}{J_h} T x_{2,k} - \frac{K_m^2 K_g^2}{R_m J_h} T x_{3,k} + \frac{K_m K_g}{R_m J_h} T u_k + x_{3,k} \tag{3.17}$$

$$x_{4,k+1} = -\frac{K_s}{J_h} T x_{2,k} + \frac{K_m^2 K_g^2}{R_m J_h} T x_{3,k} - \frac{K_m K_g}{R_m J_h} T u_k + x_{4,k} - \frac{K_s}{J_l} T x_{2,k} + \frac{MGH}{J_l} T \sin(x_{1,k} + x_{2,k}) \tag{3.18}$$

The system parameters used in this study were obtained from [11], and are summarized in the following table.

The first set of simulations were based on tracking a sinusoidal curve of amplitude 75. This corresponds to the end effector position motion. The PID gains K_P, K_I, and K_D were tuned to 4, 0.5, and 0.05 respectively. The coefficient matrix of the sliding surface was defined as $C = [0.001 \quad -1 \quad 0.1 \quad -1]$ and a fixed gain of $K_{SMC} = 200$ was used. These parameters were tuned by trial and error in an effort to improve tracking performance.

TABLE I. LIST OF MAIN SYSTEM PARAMETERS

Parameter	Symbol	Value [Units]
Spring Stiffness	K_s	1.61 N/m
Motor Constant	K_m	0.00767 $N/rad/s$
Gear Ratio	K_g	70
Inertia of Hub	J_h	0.0021 kgm^2
Load Inertia	J_l	0.0059 kgm^2
Link Mass	M	0.403 kg
Gravity Constant	G	−9.81 N/m
Height of C.M.	H	0.06 m
Motor Resistance	R_m	2.6 Ω

As shown in Figure 1, the control input for both strategies were relatively close, however the PID method had a more aggressive control signal at the start of the simulation. The desired position versus the PID and SMC results are shown in Figure 2. It is interesting to note that the PID methodology performed better in terms of tracking error near the peaks of the trajectory. The unwanted oscillations caused by the flexible-link are shown in Figure 3. The magnitude of oscillations for the PID method were about 3-4 times larger than the SMC at the beginning of the simulation. This is most likely due to the more aggressive control input. The SMC strategy was able to smooth out the magnitude of the oscillations when compared with the PID controller.

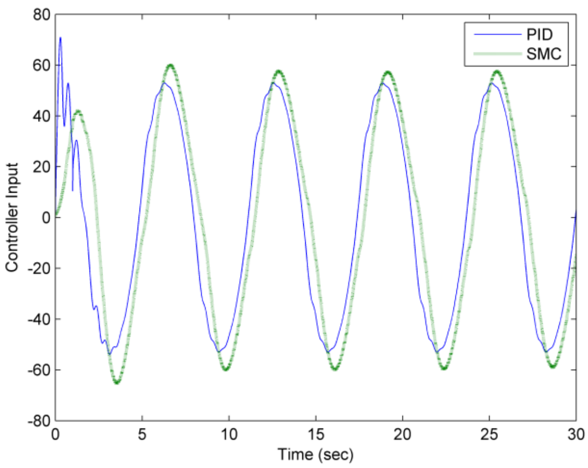

Fig. 1. PID and SMC controller inputs for sinusoidal case

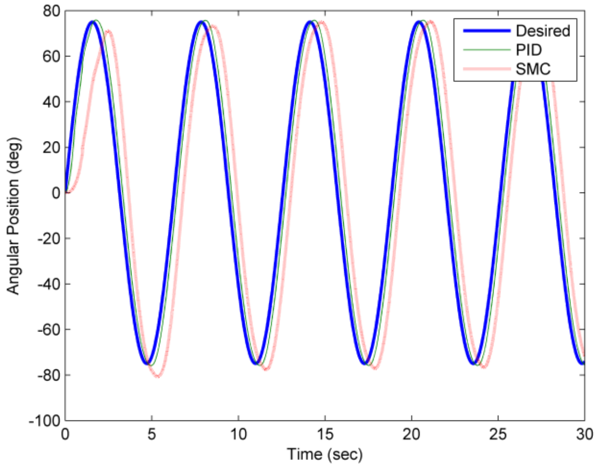

Fig. 2. PID and SMC tacking results for sinusoidal case

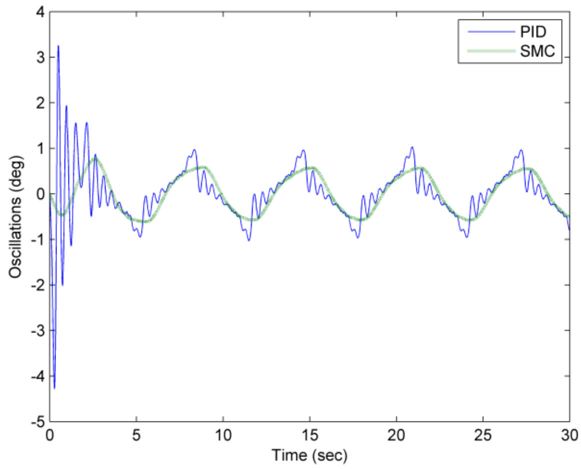

Fig. 3. Results of unwanted oscillations using PID and SMC for sinusoidal case

The second case studied a step trajectory of amplitude 75 degrees occurring at 1 second. The controller input is shown in Figure 4. The PID was significantly more aggressive at the start of the step input, however it was able to settle and yield a very good solution. The SMC method chattered significantly, and as such, the position tracking error was higher. It is interesting to note that the SMC method took longer to reach steady state, which was somewhat surprising given its robustness to rapidly changing inputs. Figure 6 shows the results of unwanted oscillations (3.16) using the PID and SMC strategies. The PID method led to unwanted oscillations of over 40 degrees at the occurrence of the step input, which is a very large value given the magnitude of the input. The SMC method limited the unwanted oscillations to within a boundary of ± 0.6 degrees. The results may have been improved further, however the same control parameters were used for both cases.

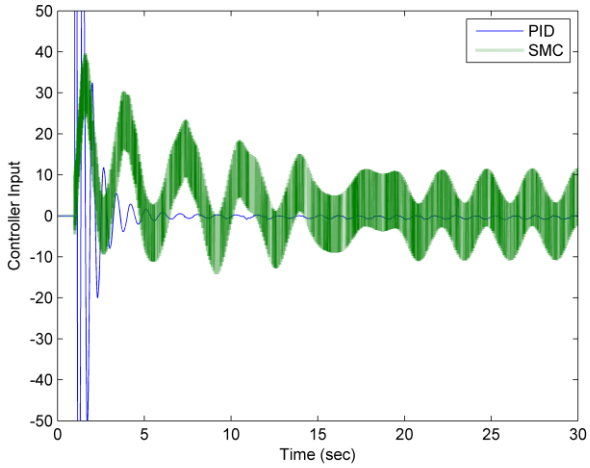

Fig. 4. Controller input values for PID and SMC for step input case

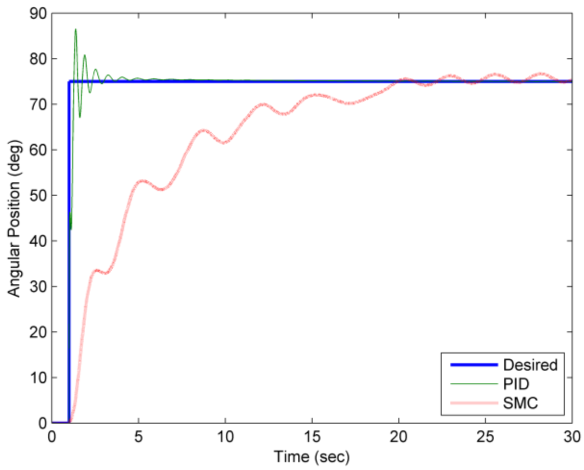

Fig. 5. PID and SMC results for step input case

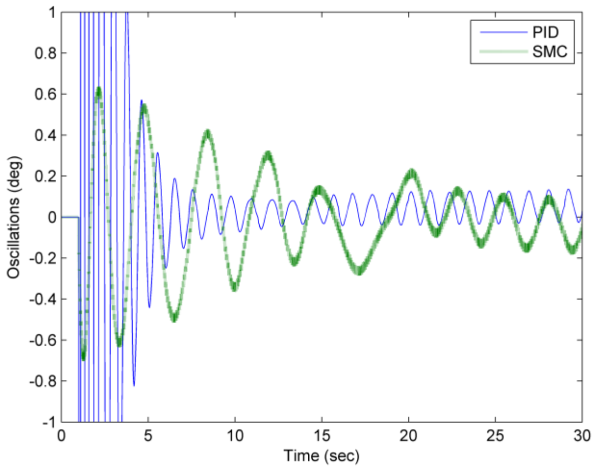

Fig. 6. Results of unwanted oscillations for step input case

5. CONCLUSION

This paper studied two popular vibration control strategies found in literature, namely the proportional-integral-derivative (PID) method and the sliding mode controller (SMC). Simulation results were generated based on applications to a flexible-link robot arm. It was the goal of the controllers to reduce unwanted vibrations at the end points caused by the elastic deflections in the link. Two cases were studied: a sinusoidal curve and a step input. It was found that the well-tuned PID controller performed very well in terms of tracking accuracy. Although the SMC strategy yielded smoother results for the first case, the PID controller provided the best solution. Future cases will study a comparison of the robustness to modeling uncertainties and system disturbances. It is expected that the SMC strategy will yield a more stable solution compared to the PID method.

6. REFERENCES

[1] I. N. Kar, K. Seto and F. Doi, "Multimode Vibration Control of a Flexible Structure using H-inf-Based Robust Control," *IEEE/ASME Transactions on Mechatronics,* vol. 5, no. 1, pp. 23-31, 2000.

[2] M. J. Balas, "Feedback Control of Flexible Systems," *IEEE Transactions on Automatic Control,* vol. 23, no. 4, pp. 673-679, 1978.

[3] M. Moallem, "Control and Design of Flexible-Link Manipulators," Ph.D. Thesis, Concordia University, Montreal, Quebec, Canada, 1996.

[4] M. Karkoub, G. Balas, K. Tamma and M. Donath, "Robust Control of Flexible Manipulators via mu-Synthesis," *Control Engineering Practice,* vol. 8, pp. 725-734, 2000.

[5] R. M. Mahamood and J. O. Pedro, "Hybrid PD/PID Controller Design for Two-Link Flexible Manipulators," in *8th Asian Control Conference (ASCC)*, Kaohsiung, Taiwan, 2011.

[6] I. Akyuz, E. Yolacan, H. M. Ertunc and Z. Bingul, "PID and State Feedback Control of a Single-Link Flexible Joint Robot Manipulator," in *IEEE International Conference on Mechatronics*, Istanbul, Turkey, 2011.

[7] M. T. Ho and Y. W. Tu, "Position Control of a Single-Link Flexible Manipulator using H-inf-Based PID Control," *IEE Proc.-Control Theory Applications,* vol. 153, no. 5, pp. 615-622, 2006.

[8] K. J. Astrom and T. Hagglund, "PID Controllers: Theory, Design, and Tuning," Instrument Society of America, Research Triangle Park, North Carolina, 1995.

[9] S. A. Gadsden and S. R. Habibi, "A New Robust Filtering Strategy for Linear Systems," *ASME Journal of Dynamic Systems, Measurements and Control,* vol. 135, no. 1, January 2013.

[10] T. Kailath, Linear Systems, Prentice Hall, 1980.

[11] K. Groves and A. Serrani, "Modeling and Nonlinear Control of a Single-Link Flexible Joint Manipulator," Department of Electrical and Computer Engineering, Ohio State University, 2014.

[12] J. J. E. Slotine and W. Li, Applied Nonlinear Control, Englewood Cliffs, NJ: Prentice-Hall, 1991.

[13] V. I. Utkin, Sliding Mode and Their Application in Variable Structure Systems, English Translation ed., Mir Publication, 1978.

[14] V. I. Utkin, "Variable Structure Systems With Sliding Mode: A Survey," *IEEE Transactions on Automatic Control,* vol. 22, pp. 212-222, 1977.

[15] S. A. Gadsden, "Smooth Variable Structure Filtering: Theory and Applications," PhD Thesis, McMaster University, Hamilton, Ontario, 2011.

[16] J. J. E. Slotine, "The Robust Control of Robot Manipulators," *International Journal of Robotic Research,* vol. 4, no. 2, pp. 49-64, 1985.

[17] J. J. E. Slotine, "Sliding Controller Design for Nonlinear Systems," *International Journal of Control,* vol. 40, no. 2, pp. 421-434, 1984.

[18] V. Jouppila, S. A. Gadsden and A. Ellman, "Experimental Comparisons of Sliding Mode Controlled Pneumatic Muscle and Cylinder Actuators," *ASME Journal of Dynamic Systems, Measurement, and Control,* 2014.